HKrF in solid krypton

Mika Pettersson,[a] Leonid Khriachtchev, Antti Lignell, and Markku Räsänen
Laboratory of Physical Chemistry, P.O. Box 55, FIN-00014 University of Helsinki, Finland

Z. Bihary
Department of Chemistry, University of California, Irvine, California 92697

R. B. Gerber
Department of Chemistry University of California, Irvine, California 92697, and Department of Physical Chemistry, The Hebrew University, Jerusalem 91904, Israel

(Received 30 October 2001; accepted 21 November 2001)

A new krypton-containing compound, HKrF, has been prepared in a low-temperature Kr matrix via VUV photolysis of the HF precursor and posterior thermal mobilization of H and F atoms. All three fundamental vibrations have been observed in the FTIR spectra at ~1950 cm^{-1} (H–Kr stretch), ~650 cm^{-1} (bending), and ~415 cm^{-1} (Kr–F stretch). Two distinct sites of HKrF have been identified. The energy difference between the H–Kr stretching vibrations for the two sites is remarkably large (26 cm^{-1}), indicating a strong influence of the environment. In annealing after the photolysis of the precursor, HKrF is formed in two different stages: at 13–16 K from closely trapped H+F pairs and at $T>24$ K due to more extensive mobility of H and F atoms in the matrix. HKrF in a less stable site decreases at temperatures above 32 K, the other site being stable up to the sublimation temperature of the matrix. The photodecomposition cross section for HKrF has been measured between 193 and 350 nm and compared with the cross sections of the previously reported HArF and HKrCl molecules. The condensed-phase VSCF (vibrational self-consistent field) calculations suggest that the more stable form is a single-substitutional site and the less stable form is a double-substitutional site of HKrF in solid Kr. The gas to matrix shifts for these sites are predicted to be $+(9-26)$ cm^{-1} for the H–Kr stretching and the bending vibrations and $-(7-10)$ cm^{-1} for the Kr–F stretching vibrations. © *2002 American Institute of Physics.*
[DOI: 10.1063/1.1434992]

I. INTRODUCTION

Chemical reactivity of rare gases is a challenging field for experimentalists as well as for theoreticians. Despite almost 40 years having passed since the preparation of the first rare-gas-containing compound,[1] recent findings indicate an emerging ''renaissance'' in this field.[2] Although a large number of Xe-containing compounds has been made, the chemistry of lighter rare gases is much more limited.[3] During the last seven years, a number of HRgY molecules (H=hydrogen; Rg=Ar, Kr, Xe; Y=fragment with large electron affinity) have been characterized experimentally in low-temperature matrixes and computationally by using *ab initio* methods.[4–11] These molecules are formed from neutral fragments,[12] and experiments support computational conclusions on their intrinsic stability versus matrix stabilization.[13] Importantly, one of the HRgY molecules, HXeI has recently been observed in Xe clusters in the molecular beam experiments.[14]

Among other HRgY molecules, two Kr-containing compounds, HKrCl and HKrCN, have been characterized.[4,6] It was understood from the early beginning of the HRgY history that the corresponding fluorides could be remarkably stable and the existence of an Ar-containing compound, HArF, was predicted.[4] Recently, the experimental preparation of HArF in an Ar matrix has been reported.[11] This remarkable observation was followed by extensive theoretical calculations on the properties of HArF and other HRgF compounds.[15,16] Interestingly, HHeF has been predicted to be a metastable molecule.[17,18] Despite the extensive calculations for the series HRgF (Rg=He, Ne, Ar, Kr, Xe, Rn),[16] only one member of this fluoride family, HArF, has up to now been experimentally characterized.[11]

In this article, we report an additional member of the HRgY family, HKrF. The observed vibrational spectrum of HKrF is compared with the existing *ab initio* calculations. In addition, the vibrational properties of HKrF in solid Kr are studied with VSCF calculations. The formation of HKrF and properties of this molecule are compared with those of the previously studied HArF and HKrCl.

II. EXPERIMENTAL DETAILS

The HF/Kr solid mixtures were studied in a closed-cycle cryostat (APD, DE 202 A) at temperatures down to 7.5 K. For a comparison, HCl/Kr and HF/Ar samples were studied under similar conditions. The samples were deposited onto a CsI or BaF_2 substrate typically kept at 20 K (Kr) or 7.5 K (Ar). The HF samples were prepared by passing Kr or Ar gas over an HF-pyridine polymer (Fluka) at room temperature. DF samples were deposited by passing HF over deuterated sulfuric acid in a deposition line. HCl samples were prepared

[a]Electronic mail: petters@csc.fi

by premixing HCl and Kr in a glass bulb. The thickness of the matrix was determined from an interference pattern of the IR spectrum being typically from 100 to 200 μm. We used Kr (99.998%), Ar (99.9999%), and HCl (99%) without additional purification. The photolysis of HF was performed by irradiating the matrix through a MgF_2 window with a Kr continuum lamp (Opthos) emitting in the 127–160 nm spectral interval. In addition, the samples were irradiated with an excimer laser (MPB, MSX-250) operating at 157 nm (F_2) or at 193 nm (ArF) and a tunable optical parametric oscillator with a frequency doubler (Continuum). The infrared spectra were measured with a Nicolet 60 SX FTIR spectrometer. In the mid-infrared region, KBr beamsplitter and a MCT detector were used, and in the far-infrared region (below 400 cm^{-1}), 6 μm mylar beamsplitter and a DTGS detector were used. The resolution of 1 cm^{-1} was used in all experiments.

III. EXPERIMENTAL RESULTS

A. Preparation and identification of HKrF

In order to prepare HKrF in solid Kr, we used our conventional procedure of solid-state synthesis: photolysis of the precursor (HF) followed by thermal mobilization of H atoms. By variation of the deposition parameters, we were able to deposit quite monomeric HF/Kr matrixes of good optical quality. The two bands of the HF monomer at 3956 and 3933 cm^{-1} dominate in IR absorption, and they are in agreement with the literature data.[19] The concentration of HF was estimated from the measured integrated absorption of monomeric HF and the thickness of the matrix, assuming that the integrated absorptivity of HF in solid Kr is the same as in the gas phase (99.8 km/mol).[20] The typical matrix ratio (Kr/HF) of ~3000 was obtained.

Both Kr lamp and 157 nm F_2 laser permanently photolyzed monomeric HF, as evidenced by the decrease of the HF absorptions. When the matrix was annealed after the photolysis, several new IR absorptions appeared as shown in Fig. 1. The strongest bands were observed at 1951.6 and 1925.4 cm^{-1}. These two bands behaved differently under annealing, as discussed later. In the lower wave number region, two weaker bands at 650.9 and 645.9 cm^{-1} with different thermal behavior appeared. In the lowest-energy region, the appearance of a band at 414.2 cm^{-1} with a shoulder at 417.0 cm^{-1} correlated with the above-mentioned absorptions. In addition to these bands, an absorption band of KrF_2 at 577.9 cm^{-1} appeared.[21] Upon deuteration of HF, the higher wave number bands shifted to 1419.1 cm^{-1} and 1401.6 cm^{-1}. The bands in the lowest-energy region shifted to 415.0 and 418.2 cm^{-1}, but the deuterated bands corresponding to the ~650 wave number region were too weak to be observed. All the relevant absorptions are collected in Table I.

The new absorption bands described above are assigned to HKrF molecules on the following basis. They are formed from the photolysis products of monomeric HF, i.e., from H and F atoms. They are specific for Kr matrixes and in solid Xe no similar absorptions appeared. In solid Ar, HArF was already previously characterized.[11] The observed absorptions agree well with the high-level anharmonic calculations of Lundell *et al.*[16] and they have proper deuteration shifts. The higher wave number bands can be assigned to the H–Kr stretch and the ~650 cm^{-1} absorptions to the bending mode. The lowest wave number absorptions are due to the Kr–F stretching vibration.

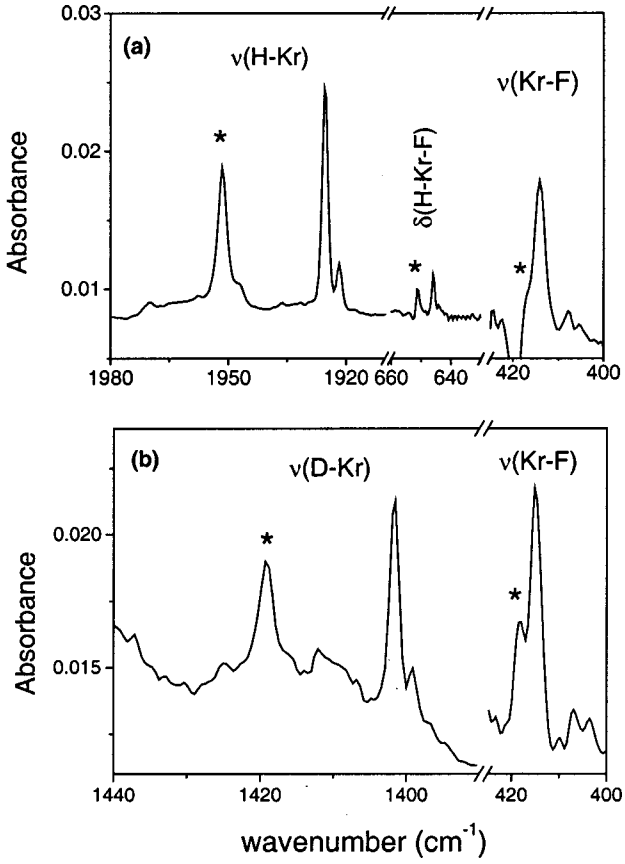

FIG. 1. IR-absorption spectra of HKrF and DKrF molecules in solid Kr. (a) HKrF absorptions showing the two sets of bands belonging to different site structures of HKrF. The absorptions marked with an asterisk belong to the $HKrF^S$ site (see the text for notation). (b) Absorptions of DKrF with $DKrF^S$ absorptions marked with an asterisk. The bending absorption was not identified for the deuterated species.

B. Two matrix sites of HKrF

In this section we concentrate on the origin of the two forms of HKrF evidenced by two different sets of bands with an appreciable shift between them. From now on we denote

TABLE I. The observed absorptions of HKrF and DKrF (in cm^{-1}). The superscript *S* or *U* refers to the site. The numbers in parentheses for the experimental values are relative intensities, including integrated absorption of both $HKrF^S$ and $HKrF^U$. For the theoretical values, the numbers in parentheses are the calculated intensities in km/mol.

	ν[H(*D*)–Kr]	δ[H(*D*)–Kr–F]	ν(Kr–F)
$HKrF^S$	1951.6 (1.0)	650.9 (0.1)	417.0 (0.6)
$HKrF^U$	1925.4 (1.0)	645.9 (0.1)	414.2 (0.6)
Theory[a]	2179.7 (122)	664.0 (10)	396.0 (216)
$DKrF^S$	1419.1 (0.7)		418.2 (1.0)
$DKrF^U$	1401.6 (0.7)		415.0 (1.0)
Theory[a]	1584.0 (64)	488.7 (2)	395.9 (216)

[a]From Ref. 16.

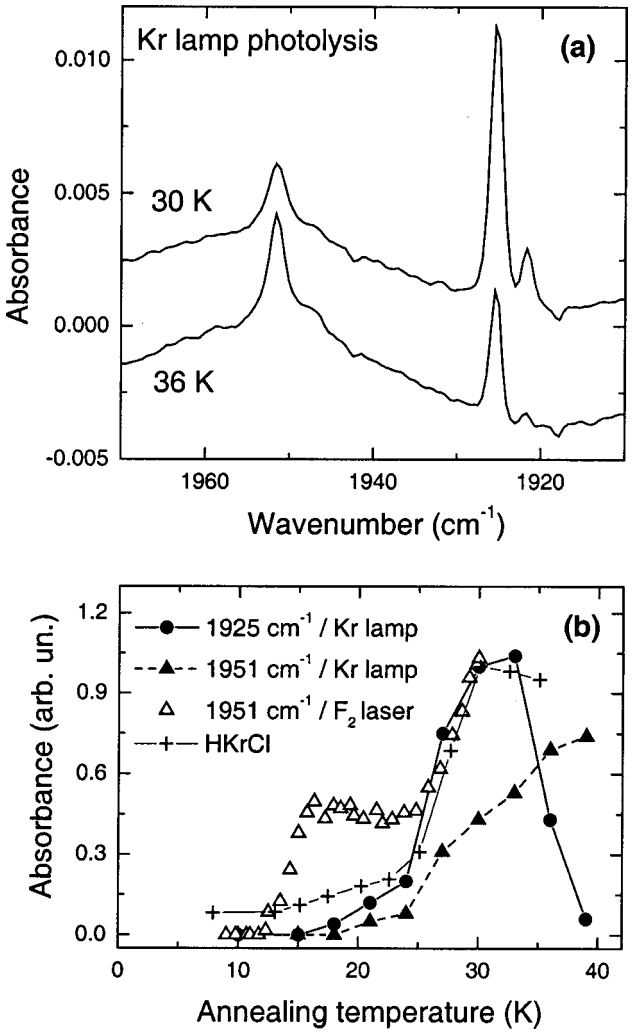

FIG. 2. Thermal behavior of different forms of HKrF. (a) The H–Kr stretching absorptions of $HKrF^S$ and $HKrF^U$ after annealing at 30 and 36 K. The spectra were recorded at 7.5 K. The data indicates the decrease of $HKrF^U$ absorption at 36 K. In (b) the integrated absorption of $HKrF^S$ and $HKrF^U$ in annealing (1 K/min) is shown. For comparison, the data for HKrCl is included in the picture.

the form with a higher wave number H–Kr stretch (1951.6 cm^{-1}) as $HKrF^S$ (*S* refers to the thermally stable form) and the form with a lower wave number H–Kr stretch (1925.4 cm^{-1}) as $HKrF^U$ (*U* referring to the thermally unstable form). Figure 2(a) shows both bands after annealing at 30 and 36 K, indicating the decrease of the $HKrF^U$ concentration at 36 K. Figure 2(b) shows the integrated band intensity of both forms as a function of the temperature in annealing (1 K/min) after the photolysis of HF. The results are shown for two matrixes irradiated with the Kr lamp and the F_2 laser featuring essential differences between the two ways of photolysis.

For the laser-irradiated (157 nm) matrixes the formation of $HKrF^S$ starts in the 13–16 K temperature interval. Between 16–24 K $HKrF^S$ is rather stable and the second formation stage starts around 25 K saturating at about 30 K. $HKrF^S$ is thermally stable and does not disappear until the sublimation of the matrix. The formation of $HKrF^S$ is different in the Kr lamp irradiated matrixes. There is no detectable low-temperature formation and the strongest increase takes place between 25 and 30 K. On the contrary, the temperature behavior of $HKrF^U$ does not depend on the irradiation wavelength. The formation starts below 20 K but the major generation takes place above 25 K similarly to the second stage of $HKrF^S$. Remarkably, $HKrF^U$ starts decomposing at about 32 K and disappears at higher temperatures. The behavior of the deuterated forms is very similar to the H forms with no significant differences in either formation or decomposition. A possible effect of the room-temperature blackbody radiation to the decomposition of $HKrF^U$ was investigated by measuring the decomposition kinetics with and without glowbar irradiation. As a result, there was no detectable effect.

For comparison, it is interesting to note that KrF_2 appeared weakly at about 13 K and increased gradually up to about 25 K. The mobility of the atomic products after HF photolysis can also be monitored from their reactions with O_2 impurity in the matrix. HO_2, which is formed from H atoms and impurity oxygen appeared already below 20 K but its major generation took place at $T>25$ K. FO_2, which forms from F atoms and O_2, shows rather similar behavior to KrF_2, i.e., it appears at about 15 K and increases up to 25 K.

C. Photodecomposition of HKrF, HArF, and HKrCl

We measured the photodecomposition cross section of HKrF, HArF, and HKrCl[22] in order to obtain information on the dissociative excited states and to make valuable comparisons between the related species. Decomposition cross section $\sigma(\lambda)$ is defined by the equation

$$dN = -\frac{N\sigma(\lambda)}{S}dn, \tag{1}$$

where N is the number of molecules, n is the number of photons, and S is the sample area. This equation establishes the way to extract the decomposition cross section at a given photon energy from the known proportion of decomposition and number of photons:

$$\sigma(\lambda) = \ln(N_0/N)S/n. \tag{2}$$

The decomposition cross sections were measured by irradiating the samples with the doubled output of the OPO. The attenuation of radiation intensity was performed by expanding the light beam with a lens. The decomposition of HRgY was followed by using the strongest H–Rg stretching bands. Figure 3 presents the cross sections as a function of the radiation wavelength. We estimate the cross sections to be correct within $\pm 50\%$. We should note that the presence of absorbing species may interfere with the measurement and lead to an underestimated cross section due to reduced beam intensity inside the sample.[23] The possible interfering species are F atoms that have absorptions in the region of HKrF and HArF absorptions. The F/Kr charge-transfer absorption has a cross section of 3.9×10^{-19} cm^2 and its maximum is at 275 nm.[24] Assuming a matrix ratio of 1/3000 and 50% decomposition for HF and the number density of Kr of 2.2×10^{22} cm^{-3}, we obtain 3.7×10^{18} cm^{-3} for the upper limit

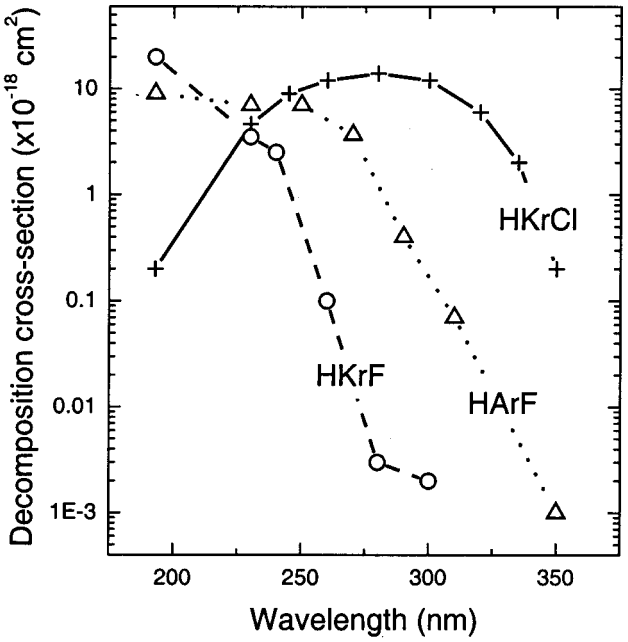

FIG. 3. The phodecomposition cross section of HKrF, HArF, and HKrCl between 350 and 193 nm. The data points were measured by tuning the photolysis laser to various wavelengths and measuring the decomposition of the molecule by FTIR spectroscopy.

of the F atom density. This gives the estimated attenuation of the beam by 1.5% for the 100 μm matrix thickness. Remembering that the decomposition cross-section measurement is made for annealed matrixes, where the number of F atoms has decreased via reactions, we can safely neglect F/Kr absorption in the measurement. Similarly, the absorption cross section for F/Ar is 1.3×10^{-18} cm^2 at 193 nm[25] and considerations similar to F/Kr, lead to the upper limit for the total attenuation of about 5% for the 100 μm matrixes. The Cl/Kr absorption maximum is at 222 nm[26,27] but, according to our knowledge, the cross section is not known. Eloranta *et al.*[28] estimated the upper limit for the cross section at 193 nm as 1×10^{-20} cm^2, which would lead to a negligible attenuation of the beam. In addition, Rayleigh scattering may lead to an overestimated cross section via increased light travel distance,[23] but its contribution is difficult to estimate quantitatively without knowing the scattering length inside the crystal.

The cross sections at the 1% level from the maximum value gives photodissociation thresholds at about 350, 300, and 250 nm for HKrCl, HArF, and HKrF, respectively. HKrCl shows a photodissociation maximum at about 280 nm and HArF and HKrF have their photodissociation maxima at $\leqslant$193 nm.

IV. SIMULATIONS

We tried to gain insight into the origin of the HKrF^S and HKrF^U by computer simulations. We calculated the vibrational spectrum of HKrF in various solid state environments. Our approach is based on a recent condensed-phase extension of the vibrational self-consistent field (VSCF) method.[29] In these simulations we calculate the vibrational spectrum of HKrF in solid krypton, taking into account anharmonicity of the potential energy surfaces and coupling between pairs of modes. It should be noted that coupling between intramolecular modes and lattice modes is also included in the description.

We used the following descriptions for the interactions in the Kr/HKrF system. The intramolecular potential is a sum of Morse potentials describing the H–Kr and Kr–F bonds, and a harmonic bending term. The parameters of this potential were fitted on the *ab initio* potential surfaces of Lundell *et al.*[16] and it reproduces the harmonic and anharmonic (VSCF) frequencies, obtained in that work, with good accuracy. We assumed the interaction between the HKrF molecule and the krypton matrix as a pairwise additive sum of interaction potentials between the molecule and the matrix atoms. In describing the molecule–matrix atom interaction, we used an electrostatic and a neutral term. The electrostatic part was calculated using the Löwdin partial charges on the atoms of the HKrF molecule, obtained by MP2 *ab initio* calculations. The neutral part was taken as a sum of atom–atom Lennard-Jones potentials, whose parameters were fitted on MP2 *ab initio* calculations and on the corresponding empirical potentials.[30,31] The Kr$\cdots$HKrF interaction obtained is anisotropic, and, compared to typical intermolecular interactions, quite strong: its well depth is $\sim$40 meV. At nearest neighbor distances, the ''electrostatic'' and the ''neutral'' parts of the interaction are of similar magnitude. This shows that the partly ionic character of the HKrF molecule, typical of the similar HRgY molecules, plays an important role in the matrix shifts. We used pairwise-additive Lennard-Jones potentials for the interaction between the matrix atoms.[32]

In the calculations, two solvation shells of matrix atoms were treated dynamically, and another two shells were frozen, simulating the crystal. We optimized the different site structures by minimizing the potential energy for the system, assuming double-substitutional (DS), and single-substitutional (SS) cavities around HKrF in the krypton lattice. For clarity, we show the relaxed configurations schematically in Fig. 4. In both sites HKrF remains linear as in the gas-phase. The DS cavity [Fig. 4(a)] is consistent with the HF occupying a substitutional site before photodissociation. The formation of this site results in some free volume, a partial vacancy on the F side [Fig. 4(a)]. The SS cavity is shown in Fig. 4(b). Its formation is consistent with the HF molecule being in an interstitial site before photodissociation, but the pictures clearly show that it can also be formed from the DS structure by a krypton atom filling the partial vacancy. It was found that the SS configuration is 3 meV lower in energy than the DS configuration.

We calculated the molecular vibrational frequencies in both relaxed configurations. The calculated frequencies and matrix shifts, together with the experimental frequencies, are summarized in Table II. The gas to matrix shifts are quite substantial, from -7 to $+26$ cm^{-1}. The discrepancy between calculated and experimental frequencies is still much higher than the matrix shifts. It shows that further refinement on the electronic structure calculations for HKrF is necessary. All the modes are stiffer for the compact SS site. The relative shifts between the DS and SS sites are in qualitative agreement with relative shifts observed in experiments between

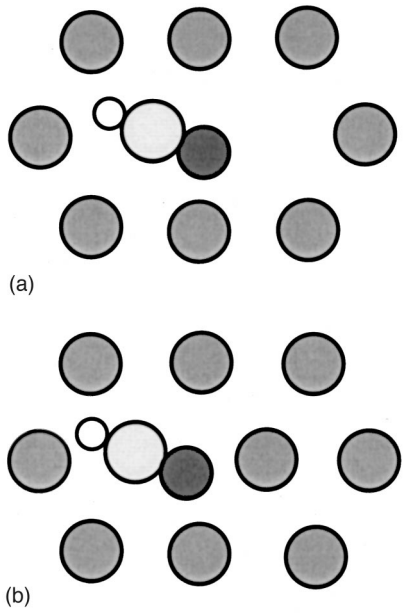

FIG. 4. The two different relaxed site configurations of HKrF in solid Kr. The DS (a) site can relax to the SS site (b) by filling of the vacancy next to the F atom by a Kr atom.

$HKrF^U$ and $HKrF^S$. This suggests that $HKrF^S$ is HKrF in a SS site and $HKrF^U$ is connected with the DS site. The disappearance of the $HKrF^U$ at $T>32$ K finds an explanation in a relaxation of the DS site to the more stable SS site by a movement of a lattice atom into a vacancy next to the F atom.

V. DISCUSSION

A. Vibrational spectrum of HKrF

The observed fundamental absorptions of HKrF are in a good agreement with the calculated values by Lundell *et al.*[16] The largest discrepancy is found between the calculated and observed H–Kr stretch being more than 200 cm^{-1}, which seems to be large, taking into account that the calculations include the anharmonic effects. The difference is most probably due to underestimated anharmonicity of the MP2 potential energy surface (PES) used in the calculations. This can be seen, for example, by comparing the H/D ratios for the H–Kr stretch. The observed ratios are 1.3748 and 1.3737 for $HKrF^S$ and $HKrF^U$, respectively, while the theoretical value is 1.3761. Additionally, as seen from the present simulations the remaining discrepancy cannot be explained by the matrix shift. These observations show that the theoretical PES is still too harmonic. The calculated and observed bending wave numbers are in a good agreement with each other. Our failure to observe the bending absorption for DKrF may be explained by the reduced intensity of this mode. The calculations predict the decrease of intensity upon deuteration by a factor of 5, which is enough to make it difficult to observe. The strong decrease of bending intensity was experimentally observed for HArF in accord with theory.[11] The Kr–F stretching absorption position is underestimated by about 20 wave numbers by calculations. More remarkable is the fact that the calculations predict a small downshift (-0.1 cm^{-1}) for the Kr–F stretch of DKrF compared with HKrF. However, in the experiments we observed an upshift by 0.8–1.2 cm^{-1}. A plausible explanation is that the calculation does not describe at a sufficient level the coupling between modes for this molecule. In this respect it is interesting to note that for HArF the calculations predict a downshift of -1.1 cm^{-1} for DArF (experimentally -0.4 cm^{-1})[11] and an upshift of $+0.5$ cm^{-1} for DXeF for the corresponding heavy-atom stretch. It can be anticipated that a more accurate anharmonic PES for HKrF with respect to the H–Kr stretch might also produce an upshift for the Kr–F stretch of DKrF.

B. Formation of HKrF

Matrix-isolated HF has some properties, different from other hydrogen halides, that are important with respect to the formation of HRgY molecules. First, monomeric HF occupies both substitutional and interstitial trapping sites in solid rare gases.[33] Second, it has been shown that both hydrogen and fluorine atoms can be thermally mobilized in solid Kr.[25,34] These two factors have important consequences concerning the distribution of the atoms and formation kinetics and site distribution of the products.

First, we discuss the photolysis of HF in substitutional and interstitial sites. The excess energy of the atoms after photodissociation at wavelengths between 127–160 nm is about 2–4 eV and partitions initially between H and F atoms. Due to the large mass difference between H and F atoms, the hydrogen can acquire most of the excess energy, and it is reasonable to assume that the hydrogen atom escapes from the parent cage. When the precursor HF occupies a substitutional site, the fluorine atom remains after the photodecomposition of HF in the substitutional site and the hydrogen atom is trapped in an interstitial site. Photolysis of interstitial HF will result in interstitial H and F atoms.

Next, we consider the formation kinetics of HKrF. The lack of the low-temperature (13–16 K) formation of $HKrF^S$ when HF is photolyzed with a Kr lamp shows that the distribution of the atoms depends strongly on the photolysis

TABLE II. Calculated vibrational frequencies and gas to matrix shifts (in parentheses), together with experimental frequencies (in cm^{-1}).

Mode	DS site (calc.)	SS site (calc.)	Difference (SS-DS)	$HKrF^U$ (Expt.)	$HKrF^S$ (Expt.)	Difference ($HKrF^S - HKrF^U$)
H–Kr stretch	2168 (+13)	2175 (+20)	+7	1925	1952	+27
Bending	685 (+9)	700 (+26)	+15	646	651	+5
F–Kr stretch	387 (−10)	390 (−7)	+3	414	417	+3

wavelength. The first formation stage of $HKrF^S$ after the 157 nm photolysis has two probable interpretations. It is formed either from closely trapped pairs of H and F atoms or it is due to extensive F atom mobility. The low-temperature formation due to global H atom mobility can be ruled out because all the evidence shows that H atoms are mobilized at higher temperatures.[34,35] Feld *et al.* showed that the fluorescence signal from F atoms decayed at ~15 K and this tends to support the interpretation based on fluorine atom mobility.[25] However, previous experiments have shown that in many cases of photolysis of small molecules in rare gas solids, a closely trapped pair of atoms is formed that can detrap at very low temperatures.[12,36,37] We call this phenomenon ''local mobility'' and find it the most probable interpretation here. Also, this image is supported by the formation kinetics of KrF_2. Although it appears in a small amount already at 13 K the major part is formed between 20 and 25 K. Moreover, FO_2 has a qualitatively similar formation mainly above 20 K. Therefore, we suggest that the low-temperature formation of $HKrF^S$ is due to local mobility of closely trapped H+F pairs. Further support to this interpretation is obtained from the HI/Xe experiments, where a closely trapped H+I configuration has been characterized.[12] In the present experiments, it is remarkable and still unclear why only $HKrF^S$, assigned to a SS site, is formed from the locally trapped configuration while $HKrF^U$ (DS site) is formed only in global H atom mobility.

The second stage of formation can be attributed to the global mobility of hydrogen atoms.[34,35] The threshold for a strong formation at ~25 K agrees with the disappearance of H atoms observed in EPR experiments and UV-absorption experiments.[34,35] In addition, we found in the present study that the formation of HKrCl behaves very similarly to HKrF at the second temperature stage [see Fig. 2(b)], which clearly supports the global H atom mobility as the origin of the formation, taking into account the immobility of Cl. The difference in the formation kinetics of $HKrF^S$ after irradiation at 157 nm (F_2 laser) or 127–160 nm (Kr lamp) fits this image and most probably has its origin in the different distribution of the atoms after photolysis, the more local distribution being connected with the less energetic photons of F_2 laser photolysis. The absence of local mobility in the case of Kr-lamp photolysis may be due to the higher excess energy of H atoms, allowing a more extensive separation of the fragments after photolysis, meaning their more efficient stabilization.

We should note here that HKrF is probably formed to some extent directly in the photolysis, but it is further photolyzed, leading to a more extensive separation of the atoms. Because of this process, the relation between the excess energy and distribution after photolysis is not straightforward. The direct formation of HKrCl in the UV photolysis of HCl in solid Kr has recently been reported, and it was shown to constitute the major channel for photolysis at 193 nm.[22] In addition, recent molecular dynamics simulations for HCl/Xe_n show that HXeCl is formed directly in the photolysis of HCl in Xe.[38] The same phenomenon was observed experimentally for HNCO/Xe[9] and HF/Ar,[11] and it is expected to be a rather general phenomenon in solid-state photodynamics.

C. Thermal decay of $HKrF^U$

We consider the decrease of $HKrF^U$ at temperatures above 32 K. The possible processes leading to the decrease include unimolecular decomposition to HF+Kr, reactions with mobile impurities, or relaxation of the environment, leading to the formation of a new solid-state configuration. Decomposition to H+Kr+F is unlikely because of a high calculated dissociation energy [1.37 eV (D_e)].[16] Unimolecular decomposition is, in principle, possible via the bending coordinate. Indeed, HKrF is estimated to be 5.15 eV higher in energy (D_e) than the HF+Kr asymptote.[16] All the computational estimates on the HRgY species have predicted substantial barriers for the decomposition via a bending coordinate. Johansson *et al.* estimated a barrier of 1.4 eV for HXeCl,[39] and Runeberg *et al.* estimated that the barrier for HArF is 1.0 eV.[15] We expect the barrier for HKrF also to be similarly high, which makes the decomposition via this mechanism improbable. In addition, it would be difficult to explain the very different stability of $HKrF^S$ and $HKrF^U$, although their bending vibrations are close, indicating similar bending potentials. The decomposition via the bending coordinate might involve tunneling and the similar behavior of HKrF and DKrF does not support the decomposition via this mechanism. Moreover, the decomposition does not involve the excitation of HKrF by blackbody radiation from the surroundings either as verified by measuring the decomposition with and without the glowbar on. Therefore we do not consider this IR-induced mechanism as a probable source of the decomposition of $HKrF^U$ above 32 K.

Reactions of HKrF with mobile atoms in the matrix is a possible source of decrease of the HKrF concentration. Both H and F atoms may react with HKrF producing H_2, F_2, and HF. However, these reactions are not expected to decompose totally $HKrF^U$ and to leave $HKrF^S$ almost intact. Therefore, although this mechanism most probably contributes to the decrease of HKrF at high temperatures, it should not be its only source.

Finally, we consider the site conversion at $T>32$ K. There are no obvious new bands appearing that can be connected with the disappearance of $HKrF^U$ and the most probable process is $HKrF^U \rightarrow HKrF^S$. Indeed, our simulations show that SS site is a lower-energy form of HKrF in solid Kr and the conversion between the sites is possible via movement of a Kr atom into a vacancy nearest to the F atom of HKrF. The only problem in this interpretation is that there is no clear one-to-one correlation between the disappearance of $HKrF^U$ and the growth of $HKrF^S$. However, if there are still mobile atoms present that can react with HKrF species, the growth of $HKrF^S$ may not be so obvious and will surely depend on the concentration and distribution of atoms. Therefore, we tentatively suggest that the disappearance of $HKrF^U$ actually involves two processes: (i) relaxation of the $HKrF^U$ configuration to $HKrF^S$ and (ii) simultaneous reactions of HKrF species with H and F atoms. This interpretation gains some support from our recent HF/Ar experiments, where similar behavior was observed and a similar model was suggested.[40] In the case of HArF, also two sites were

found, and there was a clear transformation of the unstable configuration to a more stable configuration.

The formation of HKrF in two distinct sites can be connected with the fact that the precursor HF also occupies two different sites. The photolysis prepares F atoms in substitutional and interstitial sites and the HKrF is formed in single- (from interstitial H and F and substitutional Kr) and double-substitutional (from interstitial H and substitutional F and Kr) sites. The existence of HKrF and also HArF in two different well-defined sites is a unique feature of these molecules that has not been observed for the other HRgY compounds. For XeH_2, two distinct absorption bands have been observed,[5] and this may be an indication of the existence of this molecule in two sites, similarly to HKrF and HArF.

D. Photodecomposition of HKrF, HKrCl, and HArF

Some general trends for the excited states of HRgY can be noticed from Fig. 3. When the halogen is changed from Cl to F, the excited state shifts to higher energy. Here we can also note the experiments and calculations by Ahokas *et al.* that show a similar trend for the series HXeCl, HXeBr, HXeI.[41] When the Rg is varied in HRgY, the excited states shift up when going to heavier rare gases with lower ionization potential (IP) as indicated by comparing HArF and HKrF. Here we can also compare the experimental absorption spectrum of HXeCl of Ahokas *et al.*[41] with an absorption maximum at 246 nm and the photodecomposition spectrum of HKrCl with the maximum at 280 nm.[22] Qualitatively these trends can be understood by the following model. We can consider the electronic wave function of HRgY to consist mainly of two configurations: (i) bonding HRg^+Y^- and (ii) repulsive $H^{\bullet}RgY^{\bullet}$. Asymptotically, the ionic configuration is higher in energy than the neutral one, but at shorter interatomic distances there is an avoided crossing between them and at the equilibrium configuration, the ionic configuration dominates the wave function.[10] The avoided crossing yields an excited state that is repulsive at the equilibrium configuration of HRgY. Lighter halogens favor the contribution of the ionic configuration since their small size allows a smaller distance between Rg^+ and Y^- and hence larger Coulombic stabilization. Similarly, heavier rare gases favor the contribution of the ionic configuration by lowering the energy of the $HRg^+ + Y^-$ pair at an infinite distance. As a result, the energy difference between the bound ground state and the repulsive excited state at the equilibrium geometry is increased for lighter halogens and heavier rare gases and decreased for heavier halogens and lighter rare gases. This simple model explains the observed trends in the absorption and photodissociation spectra in a qualitative way.

VI. CONCLUSIONS

A new krypton-containing compound, HKrF, has been identified in a low-temperature Kr matrix environment. HKrF is prepared by using VUV photolysis of HF in solid Kr and thermal mobilization of H and F atoms. Two distinct matrix sites are observed, and for both forms all the fundamental absorptions are reported. The assignments are confirmed by deuteration. The two sites are assigned to single-substitutional and double-substitutional configurations of HKrF in solid Kr. HKrF is formed in two temperature stages. The first one starting at 13 K is ascribed to a reaction of closely trapped H+F pairs. The second stage starting around 25 K is due to global mobility of H and F atoms. The less stable site of HKrF starts decomposing at temperatures above 32 K, the other site being stable up to sublimation of the matrix. The formation and decay of different site configurations of HKrF most probably involves thermal relaxation of the less stable site into the more stable site and secondary reactions of H and F atoms with HKrF. The simulations suggest that the more stable configuration is the single-substitutional site and the less stable configuration is the double-substitutional site. The photodecomposition cross section for HKrF has been measured between 193 and 350 nm and compared with HArF and HKrCl. Trends observed within the three systems were interpreted by a simple model, based on the roles of a repulsive neutral state and of a bonding ionic excited electronic state.

ACKNOWLEDGMENTS

Work at Helsinki was supported by the Academy of Finland. Work at UC Irvine was supported by the Chemistry Division of the National Science Foundation (NSF) (Grant No. CHE-0101199, to R.B.G.) and work at the HU was partly supported by the DFG, Germany (under Project No. Sfb 450, to R.B.G.).

[1] N. Bartlett, Proc. Chem. Soc., 218 (1962).
[2] K. O. Christe, Angew. Chem. Int. Ed. Engl. **40**, 1419 (2001).
[3] J. H. Holloway and E. G. Hope, Adv. Inorg. Chem. **46**, 51 (1999).
[4] M. Pettersson, J. Lundell, and M. Räsänen, J. Chem. Phys. **102**, 6423 (1995).
[5] M. Pettersson, J. Lundell, and M. Räsänen, J. Chem. Phys. **103**, 205 (1995).
[6] M. Pettersson, J. Lundell, L. Khriachtchev, and M. Räsänen, J. Chem. Phys. **109**, 618 (1998).
[7] M. Pettersson, J. Lundell, L. Khriachtchev, E. Isoniemi, and M. Räsänen, J. Am. Chem. Soc. **120**, 7979 (1998).
[8] M. Pettersson, L. Khriachtchev, J. Lundell, and M. Räsänen, J. Am. Chem. Soc. **121**, 11 904 (1999).
[9] M. Pettersson, L. Khriachtchev, J. Lundell, S. Jolkkonen, and M. Räsänen, J. Phys. Chem. A **104**, 3579 (2000).
[10] M. Pettersson, J. Lundell, and M. Räsänen, Eur. J. Inorg., 729 (1999).
[11] L. Khriachtchev, M. Pettersson, N. Runeberg, J. Lundell, and M. Räsänen, Nature (London) **406**, 874 (2000).
[12] M. Pettersson, J. Nieminen, L. Khriachtchev, and M. Räsänen, J. Chem. Phys. **107**, 8423 (1997).
[13] M. Lorenz, M. Räsänen, and V. E. Bondybey, J. Phys. Chem. A **104**, 3770 (2000).
[14] R. Baumfalk, N. H. Nahler, and U. Buck, J. Chem. Phys. **114**, 4755 (2001).
[15] N. Runeberg, M. Pettersson, L. Khriachtchev, J. Lundell, and M. Räsänen, J. Chem. Phys. **114**, 836 (2001).
[16] J. Lundell, G. M. Chaban, and R. B. Gerber, Chem. Phys. Lett. **331**, 308 (2000).
[17] M. W. Wong, J. Am. Chem. Soc. **122**, 6289 (2000).
[18] G. M. Chaban, J. Lundell, and R. B. Gerber, J. Chem. Phys. **115**, 7341 (2001).
[19] M. G. Mason, W. G. Von Holle, and D. W. Robinson, J. Chem. Phys. **54**, 3491 (1971).
[20] A. S. Pine, A. Fried, and J. W. Elkins, J. Mol. Spectrosc. **109**, 30 (1985).
[21] J. J. Turner and G. C. Pimentel, Science **140**, 974 (1963).
[22] L. Khriachtchev, M. Pettersson, J. Lundell, and M. Räsänen, J. Chem. Phys. **114**, 7727 (2001).

[23] L. Khriachtchev, M. Pettersson, and M. Räsänen, Chem. Phys. Lett. **288**, 727 (1998).
[24] H. Kunttu, J. Feld, R. Alimi, A. Becker, and V. A. Apkarian, J. Chem. Phys. **92**, 4856 (1990).
[25] J. Feld, H. Kunttu, and V. A. Apkarian, J. Chem. Phys. **93**, 1009 (1990).
[26] M. E. Fajardo, R. Withnall, J. Feld, F. Okada, W. Lawrence, L. Wiedeman, and V. A. Apkarian, Laser Chem. **9**, 1 (1988).
[27] K. H. Gödderz, N. Schwentner, and M. Chergui, J. Chem. Phys. **105**, 451 (1996).
[28] J. Eloranta, K. Vaskonen, and H. Kunttu, J. Chem. Phys. **110**, 7917 (1999).
[29] Z. Bihary, R. B. Gerber, and V. A. Apkarian, J. Chem. Phys. **115**, 2695 (2001).
[30] D. Schroder, J. N. Harvey, M. Aschi, and H. Schwartz, J. Chem. Phys. **108**, 8446 (1988).
[31] V. Aquilanti, E. Luzzatti, F. Pirani, and G. G. Volpi, J. Chem. Phys. **89**, 6165 (1988).
[32] C. Kittel, *Introduction to Solid State Physics*, 7th ed. (Wiley, New York, 1996).
[33] D. T. Anderson and J. S. Winn, Chem. Phys. **189**, 171 (1994).
[34] K. Vaskonen, J. Eloranta, T. Kiljunen, and H. Kunttu, J. Chem. Phys. **110**, 2122 (1999).
[35] J. Eberlein and M. Creuzburg, J. Chem. Phys. **106**, 2188 (1997).
[36] J. Eloranta, K. Vaskonen, H. Häkkänen, T. Kiljunen, and H. Kunttu, J. Chem. Phys. **109**, 7784 (1998).
[37] L. Khriachtchev, M. Pettersson, S. Pehkonen, E. Isoniemi, and M. Räsänen, J. Chem. Phys. **111**, 1650 (1999).
[38] A. Cohen, M. Y. Niv, and R. B. Gerber, Faraday Discuss. Chem. Soc. **118**, 269 (2001).
[39] M. Johansson, M. Hotokka, M. Pettersson, and M. Räsänen, Chem. Phys. **244**, 25 (1999).
[40] L. Khriachtchev, M. Pettersson, A. Lignell, and M. Räsänen, J. Am. Chem. Soc. **123**, 8610 (2001).
[41] J. Ahokas, K. Vaskonen, J. Eloranta, and H. Kunttu, J. Phys. Chem. A **104**, 9506 (2000).